

## OPTIMAL CONTROL OF VACCINE DISTRIBUTION IN A RABIES METAPOPULATION MODEL

ERIKA ASANO

Environmental Science, Policy and Geography  
University of South Florida, St. Petersburg, FL 33701

LOUIS J. GROSS

Department of Ecology and Evolutionary Biology, University of Tennessee  
Knoxville, Tennessee 37996-1610

SUZANNE LENHART

Department of Mathematics, University of Tennessee  
Knoxville, TN 37996-1300

LESLIE A. REAL

Department of Biology and Center of Disease Ecology, Emory University  
1510 Clifton Road, Atlanta, GA 30322

(Communicated by Abba Gumel)

**ABSTRACT.** We consider an SIR metapopulation model for the spread of rabies in raccoons. This system of ordinary differential equations considers subpopulations connected by movement. Vaccine for raccoons is distributed through food baits. We apply optimal control theory to find the best timing for distribution of vaccine in each of the linked subpopulations across the landscape. This strategy is chosen to limit the disease optimally by making the number of infections as small as possible while accounting for the cost of vaccination.

**1. Introduction.** Rabies is one of the oldest known viral diseases and remains the most important viral zoonotic disease world-wide. The most common mode of rabies virus transmission is through the bites of an already infected animal. Rabies virus characteristically migrates from the bite wound through the peripheral nervous system and into the central nervous system and brain. When rabies virus reaches the brain, it replicates rapidly, is shed through the salivary glands, and the infected animal starts to show signs of disease. Time between initial infection and disease onset is somewhat variable and may depend on the location and severity of wound, but infected animals usually die within a week of onset of symptoms. Although rabies vaccinations have been available for domestic animals for many years, until recently no preventive action existed to control the spread of rabies in wildlife. In the United States, wild animals accounted for 93% of reported cases of rabies in

---

2000 *Mathematics Subject Classification.* 92D30.

*Key words and phrases.* rabies in raccoons, epidemiology, mathematical model, optimal control, vaccine.

This work was supported by National Science Foundation (NSF) (Award No. ITR: 0427471) to the University of Tennessee and National Institutes of Health (NIH) grant R01 AI047498 to Emory University.

2001 [18]. Within wildlife reservoirs, several distinct rabies virus variants have been identified. There are geographically partitioned and molecularly distinguishable variants associated with different terrestrial hosts such as raccoons, skunks, foxes, coyotes, and bats [21]. However, among terrestrial animals, raccoons have been the most frequently reported rabid species (37.2% of all animal cases during 2001) and they are the primary terrestrial reservoir for rabies in the eastern United States [18].

Raccoon rabies variant emerged along the Virginia-West Virginia border in the mid 1970s and spread as an irregular wave over the eastern seaboard of the US. Raccoon rabies variant now occurs from Ontario to Alabama. The westward expansion of rabies virus in raccoons has been largely halted through the delivery of an effective oral rabies vaccine (ORV). The vaccine is a live vaccinia virus recombinant expressing the rabies glycoprotein. The live virus is embedded in a fishmeal base encased within a plastic package coated in fish meal and oil. When the raccoon eats the bait, there is an immune response to the rabies virus glycoprotein antigen, which creates antibodies to fight off the disease. Baits are distributed by fixed-wing aircraft and by truck in rural areas and by hand in urban and suburban areas. In 2003, more than 10 million baits were distributed in the United States and Canada [22].

A number of authors have explored models for control under epidemic expansion. Analytic results for optimal control applied to a simple SIR epidemic model including vaccination, quarantine, and costs for a health promotion campaign were obtained by Behncke [2]. Greenhalgh considers control of an epidemic spreading in a homogeneously mixing population, which is controlled by both immunizing susceptibles and isolating infecteds [12]. For epidemics in heterogeneous populations in which the optimal vaccination policy is linked to the changing growth rate, see the work by Cairns [3]. For deterministic and stochastic models in discrete time, describing an epidemic in an university setting, see the work by Martin et. al.[15]. Clancy treated optimal intervention policies for general stochastic epidemic models [5]. Francis [10] gives an economic analysis for a vaccination model in a flu season. Sethi, Morton, and Wickwire survey fundamental work on control of epidemics [16, 23, 24]. Ögren and Martin studied optimal vaccination patterns for a rapidly spreading disease in an urbanized, highly mobile population setting [19]. Their model is similar to one presented here but with a different spatial arrangement.

The modeling of rabies spread and control has been widely studied by ecologists and mathematical biologists. Murray, Stanley, and Brown [17] studied the spatial spread of rabies among foxes in England. In their PDE model, the fox population was divided into three classes: susceptible, infected but noninfectious, and infectious rabid [17]. Evans and Pritchard extended this model as a nonlinear time-varying control system described by partial differential equations with feedback control to drive the system toward a desired profile [7]. Coyne, Smith, and McAllister developed a model which makes explicit the development of natural immunity to rabies and used this to evaluate culling and vaccination strategies [6]. In this model, six classes were considered: susceptible raccoons, infected but noninfectious raccoons that develop rabies, infected but noninfectious raccoons that eventually develop immunity, rabid raccoons, raccoons that are immune as a result of natural infection, and vaccinated raccoons. Both discrete-time deterministic and stochastic models were analyzed by Allen, Flores, Tatnayake, and Herbold [1]. Their models are structured with respect to space ( $m$  patches), age (juvenile and adults) and three disease

states: susceptible, infected, and vaccinated. An SEIR (susceptible, exposed, infectious, and recovered) model was developed to describe the spatial and temporal patterns of raccoon rabies epizootic in [4]. Optimal control has not been previously applied to an epidemic model for rabies in raccoons; thus, this work is the first optimal control application in this area.

Rabies vaccine is distributed spatially and current distribution effort is based on guesswork and expert opinion. There is a need to develop a framework for guiding these vaccine distribution strategies. This paper is the first step toward the development of that framework and is based on spatial optimal control. This first step lays out the approach and documents the feasibility of this approach. Later papers will specifically use the techniques developed here and apply them to specific landscapes and at larger scales. In this paper, we show the success of the general approach under idealized simple landscapes. We also note that the results here are an illustration of a tool that can be adapted to other epidemic scenarios.

There are very few optimal control papers with space as a discrete variable and geographic layout. In our model, the distances in the spatial layout are shown in the movement coefficients.

Our goal is to investigate optimal vaccination strategies to control the spread of rabies using a metapopulation SIR model with a system of ODEs. In Section 2, the assumptions of our model and definitions of parameters are stated. We then give a description of our metapopulation SIR model and the objective functional to be minimized. In Section 3, we apply Pontryagin's Maximum Principle to find the necessary conditions for the optimal control. In Section 4, we show simulation results to illustrate the population dynamics with the rate of vaccination as a control. Our conclusions are given in Section 5.

**2. Metapopulation model.** We consider a population consisting of  $n$  subpopulations which are connected by immigration or emigration. Figure 1 represents the flow diagram of our model. Subpopulation  $i$  is divided into three classes; the susceptibles,  $S_i$ , that can be infected with rabies virus; the infecteds,  $I_i$ , individual raccoons that are currently infected with rabies and can transmit the virus; and the removed class,  $R_i$ , corresponding to individuals that are vaccinated and become immune to infection by rabies virus. To illustrate how control may be rapidly applied with vaccine distribution after an outbreak, we consider a short period. Natural deaths occur at a low level all year round, but birth rate occurs at a higher level during a specific time of year. Investigating the effect of seasonal birth pulse rate on vaccine distribution is important and will be considered in our future work. Because of the short period, we assume that the individuals in class  $R_i$  do not lose immunity once they are vaccinated. Our objective is to develop optimal schemes for rapid mobilization of vaccine distribution following detection of an outbreak, as this would be useful to assist in determining the best spatial distribution of effort when a surveillance program detects an outbreak.

Individuals in class  $R_i$  are removed from the system only when they die, with mortality rate  $\mu_R$ . The mortality rate for the class  $I_i$  due to rabies is much higher compared to the mortality caused by natural causes or factors other than the disease, so we only include the mortality due to rabies for the class  $I_i$ . Moreover, since the rabid animals usually die within a week after the symptoms of the disease appear, individuals in  $I_i$  do not enter the class  $R_i$ . Only the individuals in  $S_i$  can enter  $R_i$  when they are vaccinated. We do not consider the case that infected animals

recover from the disease and become immune to it, since there is little evidence for a naturally formed immune class of animals [4]. Thus, once individuals are infected, they die and are removed from the system. In Figure 1, the symbol  $a_{ij}$  represents the rate of geographic movement of uninfected individuals (susceptible and immune classes) and  $c_{ij}$  represents the rate of geographic movement of infecteds. Depending on the spatial orientation of subpopulations,  $a_{ij}$  may not be the same as  $a_{ji}$  and similarly for  $c_{ij}$  and  $c_{ji}$ . The values are assumed to be inversely proportional to the distance between the subpopulations  $i$  and  $j$ . There is some controversy about whether infected animals change their behavior, become aggressive, and move much more rapidly than uninfected ones. We can allow for the case of the movement coefficients for infecteds to be different or the same as for susceptibles. On the other hand, there are no reported alterations in behavior associated with vaccination. We assume that there is no significant change in the behavior of raccoons before and after the consumption of baits. The definition of the parameters used is summarized in Table 1.

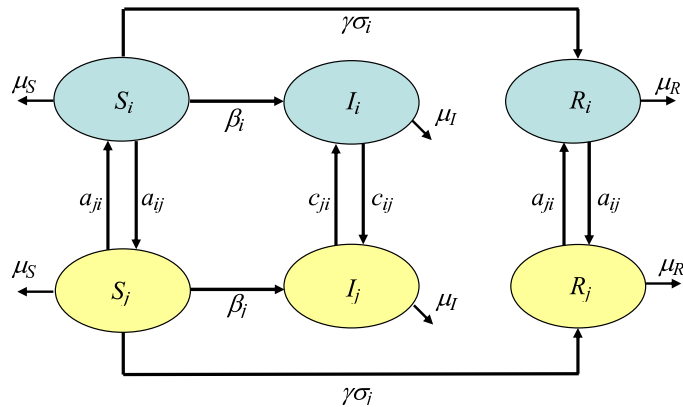


FIGURE 1. Flow diagram

Key assumptions for our model are listed below.

### Assumptions

- The mortality rates for susceptible and immune classes are the same; i.e.,  $\mu_S = \mu_R$ .
- The magnitude of the rates of geographic movement,  $a_{ij}$  and  $c_{ij}$ , reflects the distance between the subpopulations  $i$  and  $j$ . Figure 2 shows two examples of possible spatial configurations of four subpopulations from the viewpoint of subpopulation 1. In the example in Figure 2(a), the subpopulation 1 is located at the same distance from the other subpopulations 2, 3, and 4. In this case, the rates of geographic movement from  $S_1$  to the other three,  $S_2$ ,  $S_3$  and  $S_4$  are the same. However, if the distance between subpopulation 3 and subpopulation 1 is largest, as shown in Figure 2(b), then the rate  $a_{13}$  is smallest.
- If raccoons consume the baits containing the vaccine, they instantly become immune to the disease.

TABLE 1. Nomenclature

Symbol	Definition
$a_{ij}$	rate of geographic movement of noninfecteds (susceptible and immune classes) from subpopulation $i$ to subpopulation $j$
$c_{ij}$	rate of geographic movement of infecteds from subpopulation $i$ to subpopulation $j$
$\beta_i$	rate of transmission in subpopulation $i$
$\mu_S$	mortality rate for class $S$
$\mu_I$	mortality rate for class $I$
$\mu_R$	mortality rate for class $R$
$\sigma_i$	rate of vaccine bait distribution (control)
$\gamma$	efficacy of vaccination distribution
$S_i$	number of susceptibles in subpopulation $i$
$I_i$	number of infecteds in subpopulation $i$
$R_i$	number of individuals immune to the disease in subpopulation $i$

The state system is

$$\begin{aligned}
 \frac{dS_i}{dt} &= -\beta_i S_i I_i - \gamma \sigma_i S_i + \sum_{j=1, j \neq i}^n a_{ji} S_j - \sum_{j=1, j \neq i}^n a_{ij} S_i - \mu_S S_i \\
 \frac{dI_i}{dt} &= \beta_i S_i I_i + \sum_{j=1, j \neq i}^n c_{ji} I_j - \sum_{j=1, j \neq i}^n c_{ij} I_i - \mu_I I_i \\
 \frac{dR_i}{dt} &= \gamma \sigma_i S_i + \sum_{j=1, j \neq i}^n a_{ji} R_j - \sum_{j=1, j \neq i}^n a_{ij} R_i - \mu_R R_i
 \end{aligned} \tag{1}$$

$$S(0) = S_0, I(0) = I_0, R(0) = R_0.$$

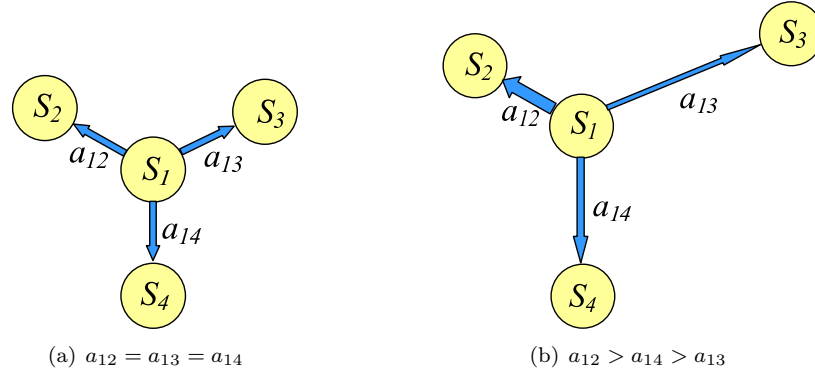
We consider this system on the time interval  $[0, T]$ . The control set is defined as

$$\begin{aligned}
 U &= \{ \sigma = (\sigma_1, \dots, \sigma_n) \mid \sigma_i \text{ is Lebesgue measurable,} \\
 &\quad 0 \leq \sigma_i(t) \leq \sigma_{\max} \text{ a.e. for } i = 1, 2, \dots, n \}.
 \end{aligned}$$

We choose the upper bound for  $\sigma$  to be 1, to represent the amount of vaccine distribution resulting from the highest level of vaccine bait distribution currently used, roughly about 150 baits/ $km^2$ . The combined coefficient  $\gamma \sigma_i(t)$  represents the rate of removal of susceptibles from subpopulation  $i$  due to vaccination. We wish to minimize the total number of infecteds and the cost associated with vaccination. We consider the following optimal control problem, for  $\sigma \in U$ .

$$\text{Minimize } J(\sigma) = \sum_{i=1}^n \int_0^T (I_i + \frac{\alpha}{2} \sigma_i^2) dt \tag{2}$$

where  $\alpha > 0$  is the weight factor in the cost of control. We choose a quadratic cost on the control for analysis convenience for this prototype problem. One can easily modify this to consider a combination of quadratic and linear cost,  $A\sigma_i + B\sigma_i^2$  where  $A > 0, B > 0$ , or other convex functions. When applying this approach to a more elaborate, realistic setting, one should choose the objective functional to more

FIGURE 2. Rate of geographic movement  $a_{ij}$ 

closely represent the actual cost and the specific goals. In a recent paper about vaccination optimal control, a cost functional of  $\sigma^{10}$  was used with justification about the big difference in cost between vaccinating at a low level compared to a high level [11].

In the next section, we show the existence of optimal controls and derive corresponding necessary conditions.

**3. Necessary conditions for the optimal control.** Note that the solutions to the state system exist and are bounded [14], independent of the control. The objective functional is convex on the compact, closed control set and the state differential equations are linear functions of the control. Using a standard result [9], we have the following existence result for an optimal control.

**THEOREM 3.1.** *There exists an optimal control  $\sigma$  in  $U$  that minimizes the objective functional  $J(\sigma)$ .*

By using Pontryagin's Maximum Principle [20, 13], we derive the necessary conditions for optimality. We form the Hamiltonian with adjoint variables  $\lambda_{1i}$ ,  $\lambda_{2i}$  and  $\lambda_{3i}$  for  $i = 1, 2, \dots, n$ .

$$H(t, S, I, R, \sigma) = \sum_{i=1}^n [I_i + \frac{\alpha}{2} \sigma_i^2 + \lambda_{1i} S'_i + \lambda_{2i} I'_i + \lambda_{3i} R'_i], \quad (3)$$

where  $\lambda_{1i}$  is multiplied by the right hand side of the  $S_i$  ODE and similarly for  $\lambda_{2i}$  and  $\lambda_{3i}$ .

**THEOREM 3.2.** *Given an optimal control  $\sigma = (\sigma_1, \sigma_2, \dots, \sigma_n)$  in  $U$  and corresponding state solutions  $S = (S_1, S_2, \dots, S_n)$ ,  $I = (I_1, I_2, \dots, I_n)$ , and  $R = (R_1, R_2, \dots, R_n)$ , there exist  $\lambda_1 = (\lambda_{11}, \lambda_{12}, \dots, \lambda_{1n})$ ,  $\lambda_2 = (\lambda_{21}, \lambda_{22}, \dots, \lambda_{2n})$ , and  $\lambda_3 = (\lambda_{31}, \lambda_{32}, \dots, \lambda_{3n})$*

satisfying the adjoint system:

$$\begin{aligned} \lambda'_{1i} &= -\frac{\partial H}{\partial S_i} = \lambda_{1i}(\beta_i I_i + \gamma \sigma_i + \sum_{k=1, k \neq i}^n a_{ik} + \mu_S) - \lambda_{2i} \beta_i I_i - \\ &\quad \lambda_{3i} \gamma \sigma_i - \sum_{k=1, k \neq i}^n \lambda_{1k} a_{ik} \\ \lambda'_{2i} &= -\frac{\partial H}{\partial I_i} = -1 + \lambda_{2i}(-\beta_i S_i + \sum_{k=1, k \neq i}^n c_{ik} + \mu_I) + \lambda_{1i} \beta_i S_j - \sum_{k=1, k \neq i}^n \lambda_{2k} c_{ik} \\ \lambda'_{3i} &= -\frac{\partial H}{\partial R_i} = \lambda_{3i}(\sum_{k=1, k \neq i}^n a_{ik} + \mu_R) - \sum_{k=1, k \neq i}^n \lambda_{3k} a_{ik} \end{aligned} \tag{4}$$

and  $\lambda_{1i}(T) = \lambda_{2i}(T) = \lambda_{3i}(T) = 0$  for  $i = 1, 2, \dots, n$ .

Furthermore we conclude

$$\sigma_i = \min\{\max\{0, \frac{\gamma S_i(\lambda_{1i} - \lambda_{3i})}{\alpha}\}, \sigma_{max}\} \text{ for } i = 1, 2, \dots, n. \tag{5}$$

*Proof.* Suppose  $\sigma = (\sigma_1, \sigma_2, \dots, \sigma_n)$  is an optimal control and  $S = (S_1, S_2, \dots, S_n)$ ,  $I = (I_1, I_2, \dots, I_n)$ , and  $R = (R_1, R_2, \dots, R_n)$  are corresponding solutions. Using the result of Pontryagin’s Maximum Principle [20], there exist adjoint variables  $\lambda_{3i}$ ,  $\lambda_{2i}$  and  $\lambda_{1i}$  satisfying: For  $i = 1, 2, \dots, n$

$$\begin{aligned} \lambda'_{1i} &= -\frac{\partial H}{\partial S_i} \\ \lambda'_{2i} &= -\frac{\partial H}{\partial I_i} \\ \lambda'_{3i} &= -\frac{\partial H}{\partial R_i} \end{aligned} \tag{6}$$

where  $H$  is the Hamiltonian, with the transversality conditions

$$\lambda_{1i}(T) = \lambda_{2i}(T) = \lambda_{3i}(T) = 0. \tag{7}$$

For example,  $\lambda'_{1i}$  for  $i = 1, \dots, n$  is given by

$$\begin{aligned} \lambda'_{1i} &= -\frac{\partial H}{\partial S_i} \\ &= \lambda_{1i}(\beta_i I_i + \gamma \sigma_i + \sum_{k=1, k \neq i}^n a_{ik} + \mu_S) - \lambda_{2i} \beta_i I_i - \lambda_{3i} \gamma \sigma_i - \sum_{k=1, k \neq i}^n \lambda_{1k} a_{ik} \end{aligned} \tag{8}$$

The general form for the optimality condition is given by

$$\frac{\partial H}{\partial \sigma_i} = \alpha \sigma_i - \gamma S_i(\lambda_{1i} - \lambda_{3i}) = 0, \text{ at } \sigma_i^* \tag{9}$$

on the set  $\{t \mid 0 < \sigma_i^*(t) < \sigma_{max}, i = 1, 2, \dots, n\}$ . By solving (9) for  $\sigma_i^*(t)$  for  $i = 1, 2, \dots, n$  on the interior of the control set, we have

$$\sigma_i^*(t) = \frac{\gamma S_i(\lambda_{1i} - \lambda_{3i})}{\alpha}. \tag{10}$$

Using the control bounds, we obtain the optimal characterization (5). □

Since the solutions of the state and adjoint systems are  $L^\infty$  bounded, the right-hand side of these ODEs are *Lipschitz* in the state and adjoint variables, which guarantees the uniqueness of the optimality system consisting of (1), (4), and (5) (with initial state and final adjoint conditions). This *Lipschitz* property implies, for  $T$  sufficiently small, the solutions of the optimality system are unique [8].

**4. Numerical results.** To illustrate our control results, we consider a population consisting of nine subpopulations whose geographical orientation is given by Figure 3. Figure 3 shows only the symmetric spatial arrangement, not the flow lines. In our examples, all nine subpopulations are connected to each other, and each movement coefficient depends solely on the distance between two subpopulations.

Since we have three state variables, susceptibles ( $S_i$ ), infected ( $I_i$ ) and removed (immune) ( $R_i$ ) for each subpopulation  $i = 1, \dots, 9$ , our state system given by (1) consists of twenty-seven ODEs. There is a corresponding system of adjoint variables consisting of twenty-seven ODEs.

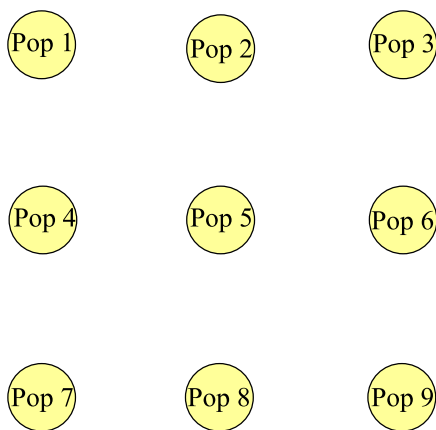


FIGURE 3. Spatial arrangement of subpopulations used in numerical simulation

We numerically solved the optimality system, consisting of fifty-four ODEs from the state and adjoint equations. Each subpopulation and the optimal control (vaccination rate) have been generated iteratively. First, we solve the state equations with a guess for the control, the state system is solved forward in time with a fourth order Runge-Kutta method. Using these state solutions, we solve the adjoint system backward in time. We repeat the iteration with the updated control (convex combination of the previous control and the value from the characterizations given by (5)) until the solutions converge.

The following is the default setting for the initial conditions and parameters. We used these values unless specified otherwise. Units are per day for all rates. We take

$$\alpha = 100$$

$$\beta_i = 0.01 \quad \text{for all } i$$

$$\mu_S = \mu_R = 0.00236, \mu_I = 0.1818.$$

$$S_i(0) = 100 \quad \text{for } i \neq 9, \quad S_9(0) = 90$$

$$I_i(0) = 0 \quad \text{for } i \neq 9, \quad I_9(0) = 10$$

$$\sigma_{max} = 1$$

$$A = (a_{ij}) = 10^{-4} \times \begin{pmatrix} 0 & 3.83 & 1.92 & 3.83 & 2.71 & 1.71 & 1.92 & 1.71 & 1.36 \\ 3.27 & 0 & 3.27 & 2.31 & 32.7 & 2.31 & 1.46 & 1.64 & 1.46 \\ 1.92 & 3.83 & 0 & 1.71 & 2.71 & 3.83 & 1.36 & 1.71 & 1.92 \\ 3.27 & 2.31 & 1.46 & 0 & 3.27 & 16.4 & 3.27 & 2.31 & 1.46 \\ 1.97 & 2.78 & 1.97 & 2.78 & 0 & 27.8 & 1.97 & 2.78 & 1.97 \\ 1.46 & 2.31 & 3.27 & 1.64 & 3.27 & 0 & 1.46 & 2.31 & 3.27 \\ 1.92 & 1.71 & 1.36 & 3.83 & 2.71 & 1.71 & 0 & 3.83 & 1.92 \\ 1.46 & 1.64 & 1.46 & 2.31 & 3.27 & 2.31 & 3.27 & 0 & 3.27 \\ 1.36 & 1.71 & 1.92 & 1.71 & 2.71 & 3.83 & 1.92 & 3.83 & 0 \end{pmatrix}$$

$$C = (c_{ij}) = aA$$

where the element,  $(a_{ij})$ , in the matrix  $A$  is the rate of movement for noninfected (susceptibles and removed (immune)) from subpopulation  $i$  to subpopulation  $j$  and similarly for  $(c_{ij})$  for the infecteds. The parameters,  $\mu_S, \mu_R, \mu_I$ , were estimated using the parameters in [6]. An estimate for  $\beta_i$  can be found in [6], but because of the short time period here, we tried a variety of values for the rate of transmission. The parameter  $\gamma$ , the efficacy of the vaccine distribution, is difficult to find in the literature, and we evaluated several different  $\gamma$  values. We can choose the coefficient,  $a$ , to adjust for differences in the movement of infected animals. We ran the simulations for  $a = 1$  and  $1.5$ .

The  $A$  values were determined in the following way. First, we assume that the population exponentially decays without birth. We determine the exponent for a simple decay model such that approximately 50% of animals will move to another subpopulation in one year (= 365 days). Of course, this percentage would be depend on the size of the regions as compared with the average home range of raccoons, so for illustration, we choose the 50% level. This can be done by solving the following equation for  $k$ ,

$$0.5S_1(0) = S_1(0)e^{-365k},$$

which gives

$$k = \frac{\ln 2}{365} \approx 1.899 \times 10^{-3}. \tag{11}$$

Next, we find the ratios of the spatial distances between subpopulation 1 and the others. Let  $l_{ij}$  denote the spatial distance between subpopulation  $i$  and  $j$ . From Figure 3, the ratios of spatial distances between subpopulation 1 and the rest of subpopulations are

$$\begin{aligned} l_{12} : l_{14} : l_{15} : l_{13} : l_{17} : l_{16} : l_{18} : l_{19} \\ = 1 : 1 : \sqrt{2} : 2 : 2 : \sqrt{5} : \sqrt{5} : 2\sqrt{2}. \end{aligned}$$

The rates of geographic movement,  $a_{ij}$  (for noninfected) and  $c_{ij}$  (for infected), are assumed to be inversely proportional to the distances between the subpopulations  $i$  and  $j$ .

We use the reciprocal of the  $l_{ij}$  and distribute the value of  $k$  to find

$$a_{1j} = \frac{1}{l_{1j}} \left( \frac{k}{\sum_{j=2}^{j=9} \frac{1}{l_{1j}}} \right).$$

Note that  $\sum_{j=2}^{j=9} a_{1j} = k \approx 1.899 \times 10^{-3}$ . Note also that  $A$  is not necessarily symmetric depending on the spatial configuration of each subpopulation with respect to each other.

By default, the initial fraction of infecteds is set to 10% of one subpopulation. In other words, if the total number in subpopulation 9 is 100 and the infection

started from this subpopulation,  $I_1(0) = 10$  and  $S_1(0) = 90$ . There are no removed (immune) individuals present at the beginning.

We discuss the results of varying certain parameters in the simulations. We changed the ratio,  $a$ , between the movement coefficients for the infected and those for the susceptibles, from 1 to 1.5. The general shape of the graphs were very similar with small changes in magnitude. If the coefficients,  $\beta_i$ , are too large, the disease spreads very fast. We choose  $\beta_i = .01$  for illustration. (Note for a more realistic case, one could choose different values for  $\beta_i$  in different subpopulations to represent different conditions.) If we changed  $\gamma$  to be a lower value than .4, this results in a corresponding lower level of vaccine control. Note that for all the simulations, the time period is 15 days. We are thus considering a very brief period following a serious outbreak. First we show the simulation results for two different  $\gamma$  values.

**Example 1**  $\gamma = .4$ : The numbers in each class (susceptibles (solid line), infected (dotted line) and removed (dashed line)) are shown in Figure 4(a), and the optimal control (vaccination rate) is shown in Figure 4(b). The numbers in each class for the whole population are shown in Figure 5.

Because of the spatial symmetry of the subpopulations, both the final time population distribution and the optimal control(vaccination) are symmetric. The vaccine graphs are the same for pairs 2 and 4, 3 and 7, and 6 and 8. If one compares the actual vaccine values for different pairs, the numbers are slightly different.

Larger values of  $\alpha$  mean the cost associated with vaccination is larger; thus, we expect that less control(vaccination) will be applied for larger  $\alpha$ . We verified this by considering  $\alpha = 50, 100, 200$ . For all three cases, the infecteds in the subpopulation 9 die out, since there are not enough susceptible raccoons present.

For reference, the numbers in the susceptible and infected classes starting with the same initial populations without control are shown in Figure 8(a). The numbers in each class for the whole population are shown in Figure 8(b). There are no removed in this case. Without vaccination, rabies spreads quickly to wipe out the population.

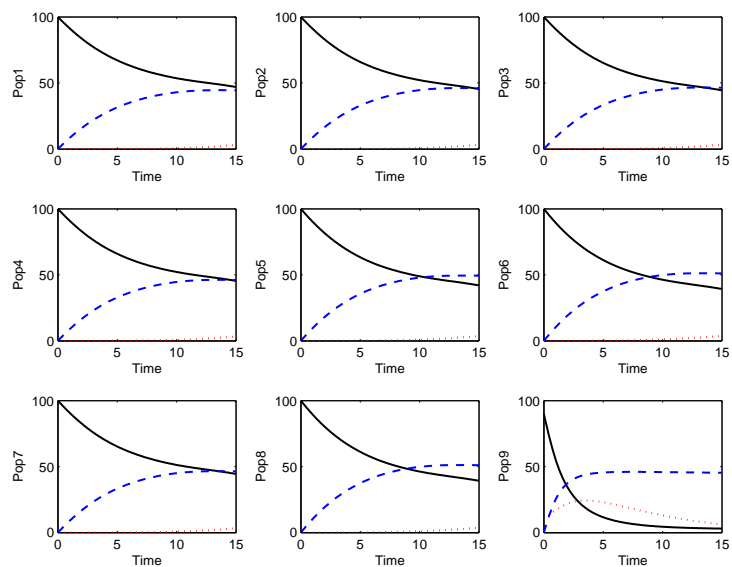
**Example 2**  $\gamma = .1$ : In this example, only the efficacy of vaccination distribution,  $\gamma$ , is changed from 0.4 to 0.1. The numbers in each class and the optimal control are shown in Figure 6. The numbers in each class for the whole population are shown in Figure 7. The numbers in susceptible in subpopulation 9 decrease similarly for both cases, but for lower value of  $\gamma$ , there are more immunes and less infecteds.

The different sizes and location of the initial subpopulations seems to be a crucial feature. Next, we examined varying the initial population.

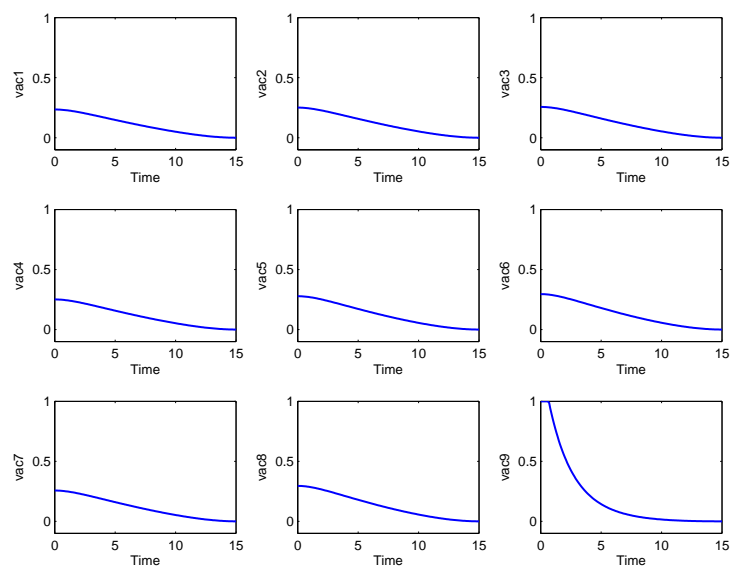
**Example 3**  $\gamma = .1$ :

$$\begin{aligned} S_1(0) &= S_6(0) = S_9(0) = 100, \\ S_2(0) &= S_5(0) = 50, S_3(0) = 150, S_4(0) = 45, \\ S_7(0) &= 250, S_8(0) = 200, \\ I_4(0) &= 5. \end{aligned}$$

The origin of the spread is subpopulation 4. The numbers in each class (susceptibles, infected, and removed) are shown in Figure 9(a). The onset of the spread is much faster in large subpopulations. In this example, five infecteds are introduced in subpopulation 4. The animals move out to either subpopulation 1 or subpopulation 7 with equal rates. However, the number of infecteds in the larger subpopulation



(a) Population  $S$ (solid),  $I$ (dotted),  $R$ (dashed)



(b) Optimal control

FIGURE 4. Population distribution and optimal control with  $\gamma = .4$ ,  $I_9(0) = 10$  (Example 1).

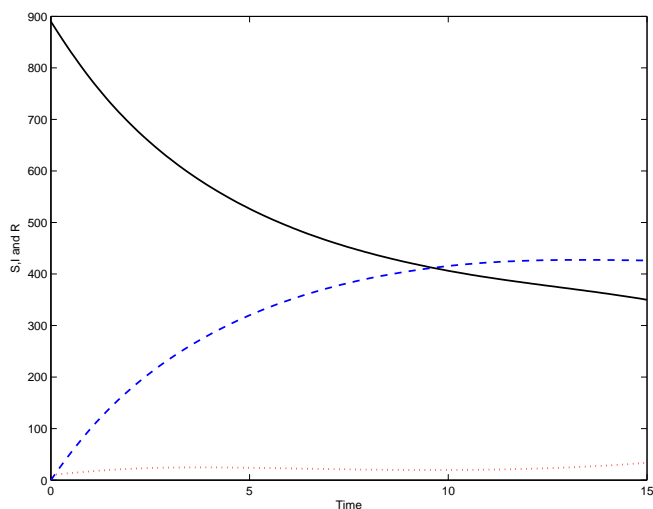


FIGURE 5. Total population with  $\gamma = .4$ ,  $I_9(0) = 10$  (Example 1).  $S$ (solid),  $I$ (dotted),  $R$ (dashed).

7 started increasing earlier than that in subpopulation 1. Moreover, subpopulation 5 is closer to the origin of the spread, subpopulation 4, than subpopulation 3, but the spread is faster in subpopulation 3, where more susceptibles are present. The numbers in each class for the whole population are shown in Figure 10.

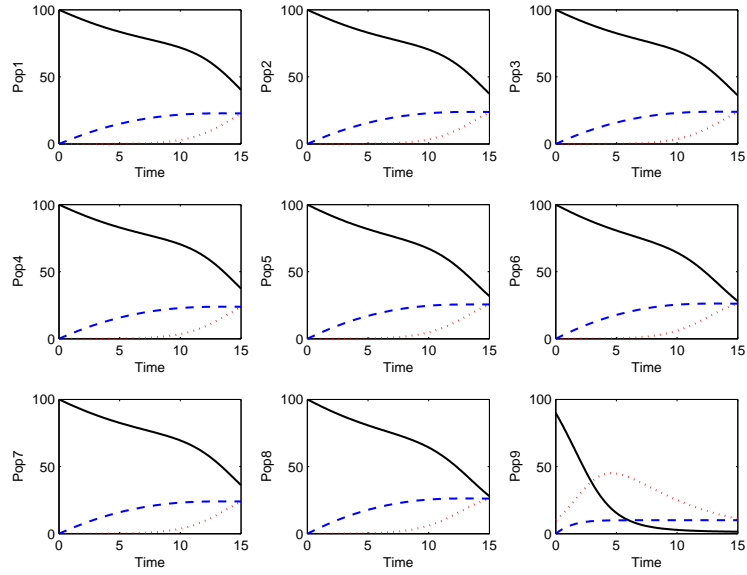
Examining the optimal control shown in Figure 9(b), we see more control (vaccination) is applied in larger subpopulations, such as subpopulations 3, 7, and 8. Almost no control is applied for the much smaller populations such as 2 and 5. As before, without control, the population will rapidly die.

**Example 4)**  $\gamma = .1$ . In this example, only the origin of the spread is changed. Instead of subpopulation 4, we started with the infected individuals in subpopulation 7. Note that the number of infected is 25 (10% of the total number). The only change from the last example is the following.

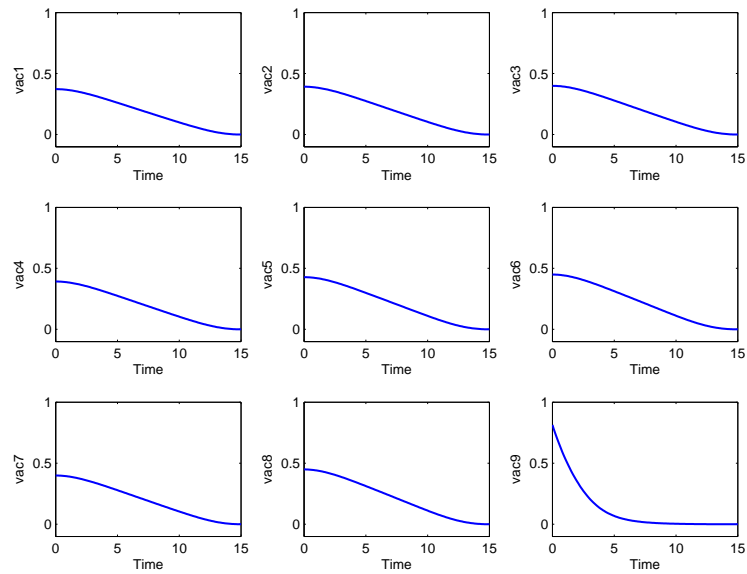
$$S_4(0) = 50, S_7(0) = 225, I_7(0) = 25.$$

The results are shown in Figures 11 and 12. As in the last example, the strategy to minimize the objective functional is to vaccinate the populations large in size. In this example, the infection started in the largest subpopulation. Since the susceptibles in subpopulation 7 are quickly infected, the intensity of the control is much less than that of the previous example. Again, if the population size is relatively large, the vaccination rate is very high.

**5. Conclusions.** We constructed a metapopulation SIR (susceptible, infected, and removed(immune)) model to investigate optimal vaccination strategies to control rabies among raccoons over a short-term time period. It is a system of  $3n$  ODEs ( $n$  is the number of subpopulations). This model and the control techniques could easily be adapted to other epidemics than rabies. This work provides a useful tool for analyzing optimal control in metapopulation epidemic models.



(a) Population  $S$ (solid),  $I$ (dotted),  $R$ (dashed)



(b) Optimal control

FIGURE 6. Population distribution and optimal control with  $\gamma = .1$ ,  $I_9(0) = 10$  (Example 2).

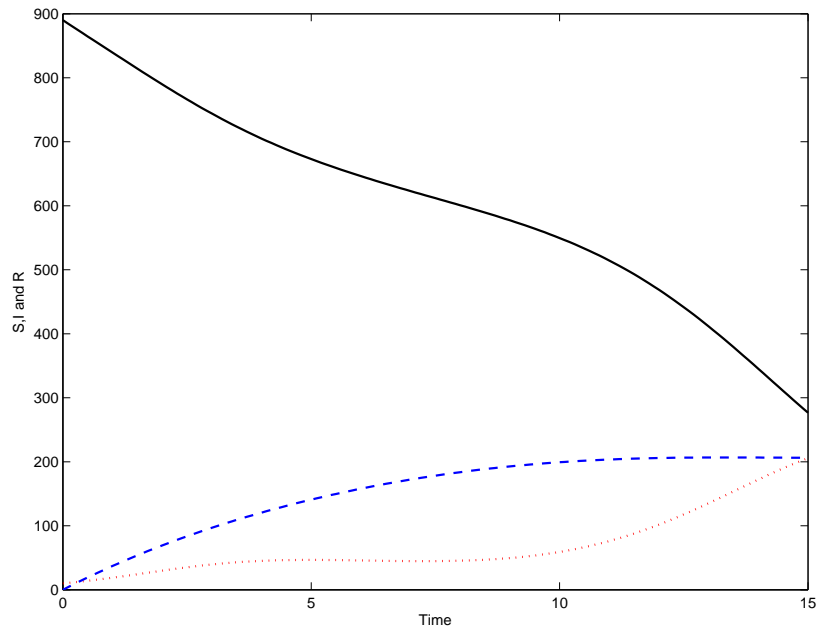


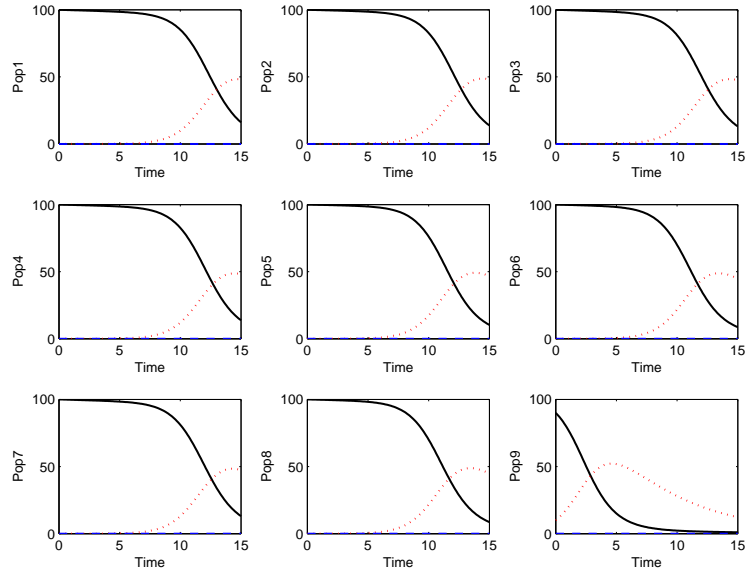
FIGURE 7. Total population with  $\gamma = .1$ ,  $I_9(0) = 10$  (Example 2).  $S$ (solid),  $I$ (dotted),  $R$ (dashed).

We have developed the necessary conditions for the optimal control using the Pontryagin's Maximum Principle. Using the state and adjoint system together with the characterization of the optimal control, we solved the problem numerically with a variety of parameter values.

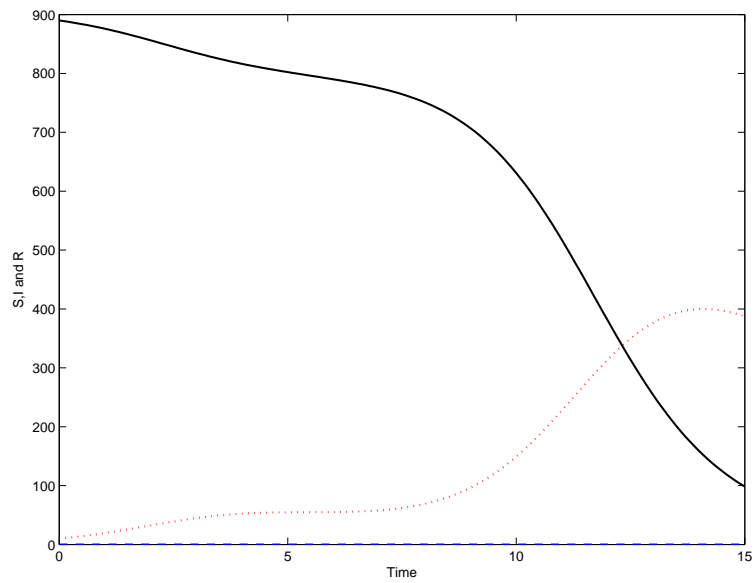
For the case of nine subpopulations, the optimal strategy is to vaccinate at a higher rate in larger subpopulations. When the cost of applying the vaccine is higher, as expected, the amount of effort devoted to vaccination is lower. This can also be seen in the graphs for the total population. These control results illustrate how the spatial arrangement and the location of the initial infecteds can affect the optimal vaccination strategy.

When we compare the numbers of each class for the whole populations in examples 1 and 2 (different  $\gamma$  values), the case with higher  $\gamma$  values (example 1) shows that the number of the infecteds stays low all the time. On the other hand, when the efficacy of vaccination is lowered, the number of infecteds starts rising around day 10 and keeps increasing to reach 200 after at day 15.

When the initial number of each subpopulation is different (examples 2 through 4), the pattern of the change in the total number of infecteds depends on the size of the subpopulation where the initial infected animals were introduced. In example 2 (see Figure 7), there is a slight increase in the number of infecteds, but the number remains low until it gradually increases around day 10. In example 3 (see Figure 10), the number of infecteds begins to increase around day 5; then the rate of increase slows down as the number of susceptibles decreases. Even though the initial number of infecteds in example 3 is less than in example 2, the number of infecteds reaches

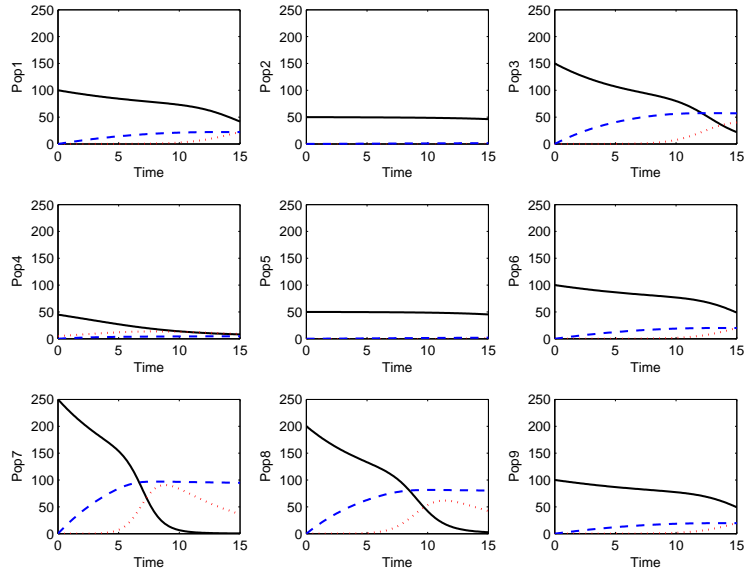


(a) Population distribution  $S$ (solid),  $I$ (dotted)

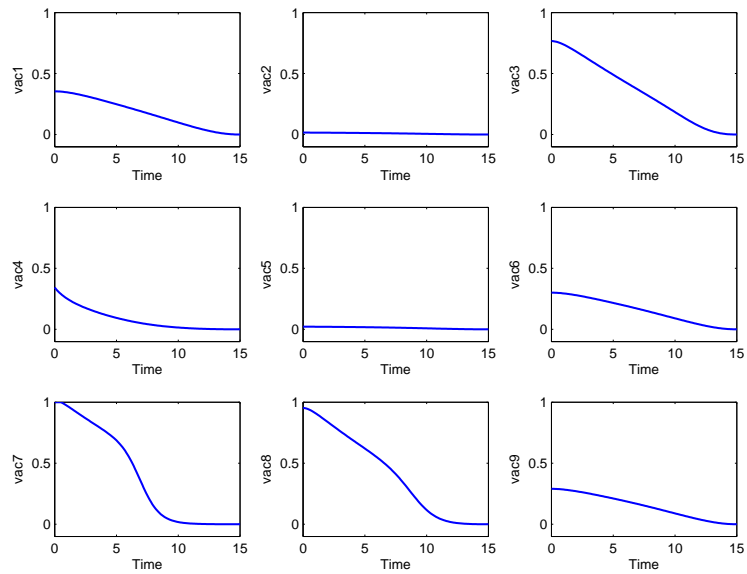


(b) Total population distribution

FIGURE 8. Population distribution without control (Examples 1 and 2).  $S$ (solid),  $I$ (dotted).



(a) Population  $S$ (solid),  $I$ (dotted),  $R$ (dashed)



(b) Optimal control

FIGURE 9. Population distribution and optimal control with  $I_4(0) = 5$  (Example 3).

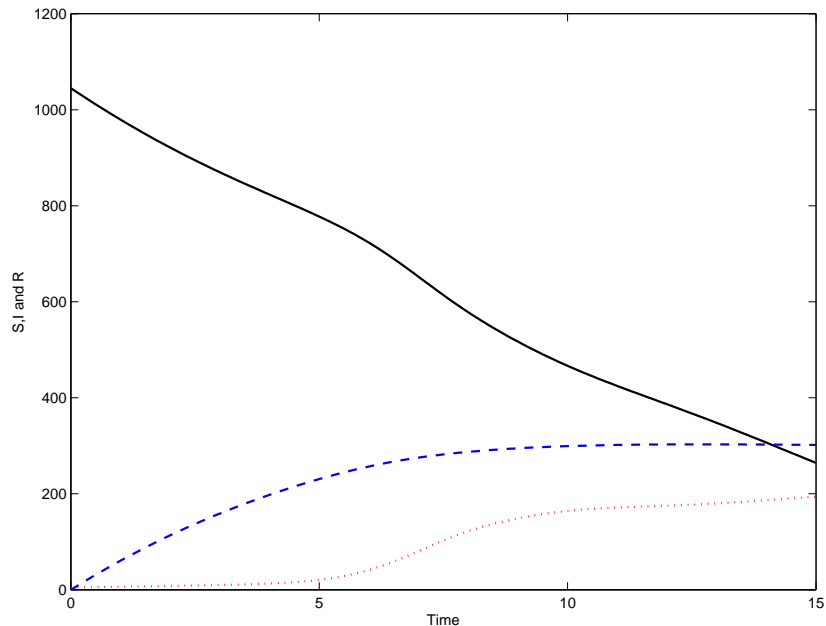


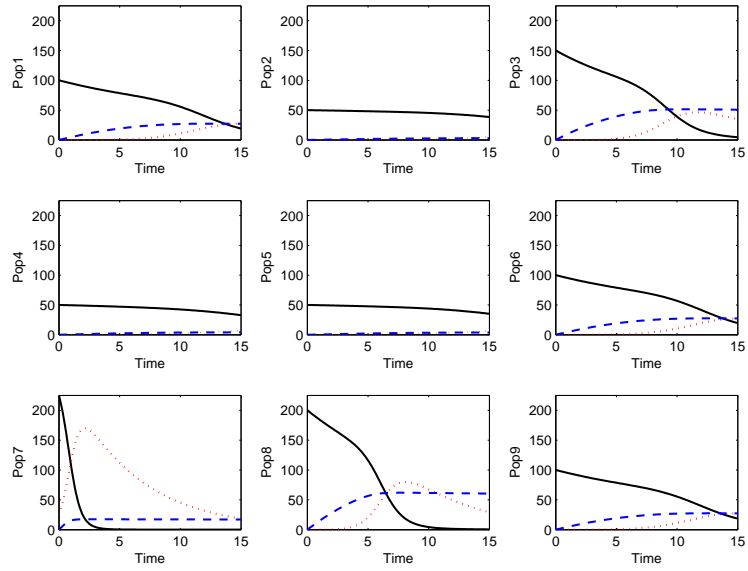
FIGURE 10. Total population with  $I_4(0) = 5$  (Example 3).  $S$ (solid),  $I$ (dotted),  $R$ (dashed).

approximately 100 by day 8, whereas it takes about 12 days in example 2. When the initial infecteds are placed in relatively large size subpopulation as in example 4, the number of infecteds increases quickly at the beginning and does not change much after that (see Figure 12).

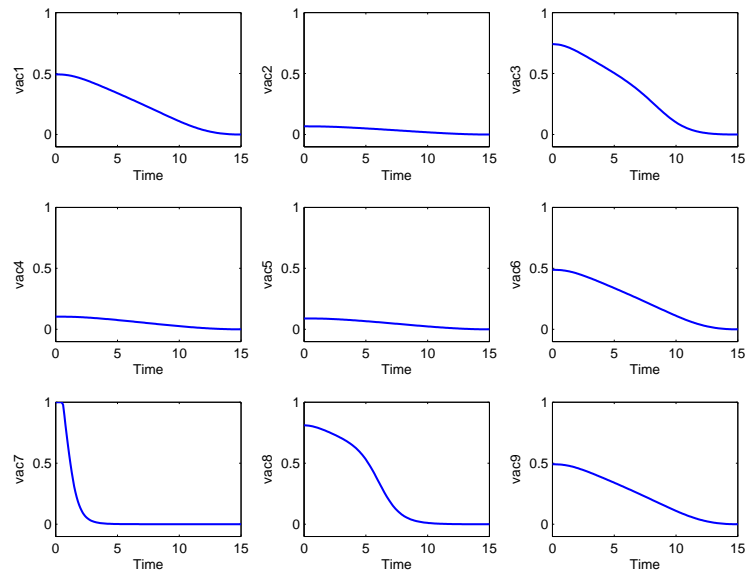
Note also that convergence of the iterative method to find the optimal control was quick and this indicates that problems with even much more refined spatial grids could be handled readily.

The following is a list of some features which could be added to increase the predictive power of the model for decision making by policy agencies.

- Introduce another state variable to add the dynamics of the bait, since the baits are delivered at different spatial locations and may decay over time or be consumed by other animals.
- Add another class, exposed (latently infected),  $E$ , which represents the group of individuals who are infected but do not transmit the disease yet. This extension would be particularly relevant if the time period for the analysis were taken to be longer than the period immediately following an outbreak we consider here.
- Include birth and growth terms, including possibly a birth pulse function or maturity movement function, in the state equations.
- Add more constraints such as a limit on the amount of vaccine to be used.
- Add age or gender structures (adult/juvenile/male/female).
- Use more realistic parameter values and geographic layout.



(a) Population  $S$ (solid),  $I$ (dotted),  $R$ (dashed)



(b) Optimal control

FIGURE 11. Population distribution and optimal control with  $I_7(0) = 25$  (Example 4).

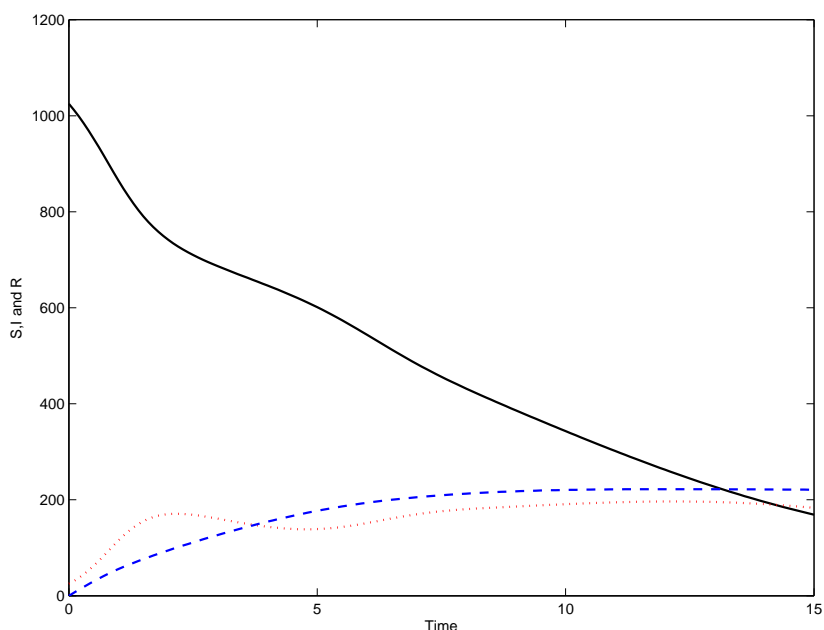


FIGURE 12. Total population with  $I_7(0) = 25$  (Example 4).  $S$ (solid),  $I$ (dotted),  $R$ (dashed).

#### REFERENCES

- [1] L. J. S. Allen, D. A. Flores, R. K. Ratnayake, and J. R. Herbold. Discrete-time deterministic and stochastic models for the spread of rabies. *Applied Mathematics and Computation*, 132:271–92, 2002.
- [2] H. Behncke. Optimal control of deterministic dynamics. *Optim. Control Appl. Meth.*, 21:269–85, 2000.
- [3] A. J. G. Cairns. Epidemics in heterogeneous populations: aspects of optimal vaccination policies. *IMA J. of Math. Applied to Med. and Biology*, 6:137–59, 1989.
- [4] J. E. Childs, A. T. Curns, M. E. Dey, L. A. Real, L. Feinstein, and O. N. Bjornstad. Predicting the local dynamics of epizootic rabies among raccoons in the United States. *PNAS*, 97(25):13666–71, 2000.
- [5] D. Clancy. Optimal intervention for epidemic models with general intervention and removal rate functions. *J. Math. Biol.*, 39:309–31, 1999.
- [6] M. J. Coyne, G. Smith, and F. E. McAllister. Mathematic model for the population biology of rabies in raccoons in the mid-Atlantic states. *American Journal of veterinary research*, 50(12):2148–54, 1989.
- [7] N. D. Evans and A. J. Pritchard. A control theoretic approach to containing the spread of rabies. *IMA Journal of Mathematics Applied in Medicine and Biology*, 18:1–23, 2001.
- [8] R. Fister, S. Lenhart, and J. S. McNally. Optimizing chemotherapy in an HIV model. *Electronic Journal of Differential Equations*, 1998(32):1–12, 1998.
- [9] W. H. Fleming and R. W. Rishel. *Deterministic and Stochastic Optimal Control*. Springer-Verlag, New York, 2005.
- [10] P. J. Francis. Optimal tax/subsidy combinations for the flu season. *J. of Econ. Dynamics and Control*, 28:2037–54, 2004.
- [11] H. Gaff and E. Schaefer. Optimal control applied to vaccination and treatment strategies for various epidemiologic models. preprint.

- [12] D. Greenhalgh. Some results on optimal control applied to epidemics. *Math. Biosci.*, 88:125–58, 1988.
- [13] M. I. Kamien and N. L. Schwarz. *Dynamic Optimization: The Calculus of Variations and Optimal Control in Economics and Management*. North-Holland, Amsterdam, 1991.
- [14] D. L. Lukes. *Differential Equations: Classical to Controlled, Mathematics in Science and Engineering*, volume 162. Academic press, New York, 1982.
- [15] C. Martin, L. Allen, M. Stamp, M. Jones, and R. Carpio. A model for the optimal control of a measles epidemic. In *Computation and Control II, Proceedings of the Third Bozeman Conference*, pages 265–83, Boston, 1992. Birkhauser.
- [16] R. Morton and K. H. Wickwire. On the optimal control of a deterministic epidemic. *Advances in Appl. Probability*, 6:622–35, 1974.
- [17] J. D. Murray, E. A. Stanley, and D. L. Brown. On the spatial spread of rabies among foxes. *Proc. R. Soc. London B*, 229:111–50, 1986.
- [18] Division of Viral and Rickettsial Diseases (DVRD). Rabies. From National Center for Infectious Diseases (NCID) web site concerning rabies (<http://www.cdc.gov/ncidod/dvrd/rabies/>). Centers for Disease Control and Prevention.
- [19] P. Ögren and C. F. Martin. Vaccination strategies for epidemics in highly mobile populations. *Applied Mathematics and Computation*, 127:261–76, 2002.
- [20] L. S. Pontryagin, V. G. Boltyanskii, R. V. Gamkrelize, and E. F. Mishchenko. *The Mathematical Theory of Optimal Processes*. Wiley, New York, 1962.
- [21] L. A. Real, C. Russell, L. Waller, D. Smith, and J. Childs. Spatial dynamics and molecular ecology of north American rabies. *Journal of Heredity*, 96(3):253–60, 2005.
- [22] USDA Wildlife Services. National Rabies Management Program. From USDA Animal and Plant Health Inspection Service web site concerning the National Rabies Management Program (<http://www.aphis.usda.gov/ws/rabies/>). USDA Animal and Plant Health Inspection Service.
- [23] S. P. Sethi. Quantitative guidelines for communicable disease control program: a complete synthesis. *Biometrics*, 30:681–91, 1974.
- [24] K. Wickwire. Mathematical models for the control of pests and infectious diseases: a survey. *Theoretical Population Biology*, 11:182–238, 1977.

Received on July 11, 2007. Accepted on February 11, 2008.

*E-mail address:* `easano@stpt.usf.edu`

*E-mail address:* `lenhart@math.utk.edu`

*E-mail address:* `gross@tiem.utk.edu`

*E-mail address:* `lreal@emory.edu`